Journal of Nuclear Materials 92 (1980) 2–25

LIQUID METAL EMBRITTLEMENT OF NUCLEAR MATERIALS

C.F. OLD
UKAEA, Materials Development Division, Atomic Energy Research Establishment, Harwell, Oxfordshire OX11 0RA, UK

Received 17 April 1980

The phenomenological features of liquid metal embrittlement (LME) are reviewed and the influence of metallurgical factors and testing conditions is described. The process is shown to be similar in many respects to the elastic fracture observed at lower temperatures in some bcc and hcp. metals. An important difference in the case of LME arises from the need for the embrittler to be present at the crack-tip during fracture. This condition imposes a low temperature limit which occurs when the embrittler is no longer mobile. The relationship between susceptibility to LME and alloying characteristics is discussed. The various theories have been considered and it is concluded that a reduction in surface energy leading to lower crack-tip cohesion and hence lower plastic deformation is consistent with most of the experimental evidence.

The second section of the review uses this general understanding as a basis for speculation about possible synergy between LME and radiation effects. Those which alter the plastic deformation behaviour, i.e., radiation hardening or radiation annealing, are considered likely to have the same influences on embrittlement as on elastic fracture. Radiation creep will reduce any tendency to slow crack growth under restricted embrittler availability. Radiation-induced transmutation is seen as a possible source of supply of embrittling species, particularly as fission products, but interaction with high temperature creep-cavitation fracture by helium segregation is less likely because LME tends to be more severe at lower temperatures.

The review concludes with a brief catalogue of LME-susceptible couples, concentrating as far as possible on nuclear materials (i.e. ferrous and zirconium alloys) to provide an initial source of data for materials selection by designers and operators and for failure analysis.

1. Introduction

The embrittlement of otherwise ductile metals stressed in contact with liquid metals has been known for at least sixty years [1]. Despite its long history, however, it is still not well understood and laboratory experiments show that it is sensitive to both materials and testing conditions. Many materials are known to be susceptible. For example, ferrous alloys ranging from pure iron to austenitic stainless steels are variously reported to be embrittled by one or more of the liquid metals bismuth, gallium, mercury [2], cadmium [3], copper [4], indium [5], lithium [6], lead [7], tin and zinc [8]. Apart from its scientific interest as an example of environmental fracture, it is thus also technologically important as a failure mode in engineering structures [9–11].

Since nuclear technology shares many materials and techniques with more conventional engineering, it is appropriate to consider the interaction of those factors which are peculiar to nuclear applications with the embrittlement process. The use of liquid alkali metal coolants in fast fission and the proposed fusion reactor lends added point to the study. To the best of the author's knowledge, there are no reports of any generic work on the effect of such factors and thus their influence can only be estimated from a comparison with existing data and an understanding of the mechanism of embrittlement.

This review therefore begins by describing the phenomenological features of liquid metal embrittlement (LME), and then goes on to interpret these features in the context of a brittle-fracture mechanism. This is followed by a consideration of the effects of the nuclear environment on materials behaviour and some speculative comments are offered as to how those effects might alter the occurrence and severity of embrittlement. Finally, the review provides a brief survey of the available information on the embrittlement of those materials of special

interest in the nuclear field, i.e., principally steels and zirconium alloys.

2. Phenomenological behaviour of LME

2.1. Failure mode

There are several mechanisms by which a liquid metal may degrade a solid metal. Some liquid metals such as aluminium are reactive and will attack and erode many other metals with the formation of intermetallic compounds. In other combinations, the attack is confined to a particular phase or constituent of a solid alloy. For instance, above 750°C zinc preferentially dissolves the nickel in the grain boundary regions of austenitic stainless steels [12], while lithium reduces grain-boundary carbides in carbon steels [13]. In more inert systems, degradation of the solid may still occur through grain-boundary penetration by the liquid metal; solid polycrystalline zinc and aluminium disintegrate into separate grains even when unstressed after a period in contact with liquid gallium at 30°C [14,15]. Yet a further route involves the liquid metal acting as a transport medium for impurities or other alloying elements where chemical activity gradients occur and thus permitting structural or compositional changes (e.g. sodium in steel containments).

The classical liquid metal embrittlement discussed in this review shows important differences from the processes described above. LME requires a critical strain and degradation is not progressive. Thus failure is equally likely after a short or long exposure and it is not possible to estimate a conservative useful life based upon the length of contact-time. If the liquid metal embrittler is immobilised by freezing or removed before the critical stress is applied, then the mechanical properties of the solid are unaffected. In addition, embrittlement is often restricted to a limited temperature range. This has important technological implications because it prevents the identification of susceptible systems by simple high temperature screening tests carried out on the assumption that higher temperatures are likely to exacerbate any detrimental effects.

Fracture by LME in polycrystals generally occurs by fast crack propagation, leading to frequent references to "instant" or "catastrophic" failure. Failure is often intergranular, although transgranular quasi-cleavage is sometimes observed and single crystals can also be embrittled [16–18]. Moreover, some systems are susceptible to other forms of liquid metal degradation as well as classical LME. For example, while aluminium polycrystals are severely embrittled by gallium and fail at strains of 1% or less, they also suffer grain boundary penetration by gallium in the absence of stress. Somewhat similar effects are exhibited by some ferrous alloys in the presence of zinc and lithium. This combination can make the identification of LME difficult and thus care is needed to define the precise mode of failure.

2.2. Conditions for LME in susceptible systems

A minimum strain and intimate contact between solid and liquid metals must exist simultaneously before failure will occur. The minimum strain can vary widely and in extreme cases can be <1% [19]. Until fracture occurs, the stress–strain behaviour of the solid metal is the same as that in the unwetted condition [20] (fig. 1). Some authors claim that embrittlement occurs immediately when the liquid metal is applied to a specimen stressed above a certain threshold level. However, Hancock and Ives [21]

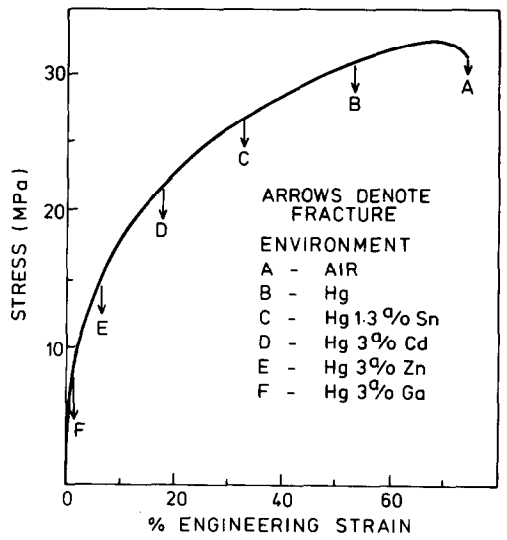

Fig. 1. Progressive curtailment of unique stress–strain curve of pure aluminium tested in air, mercury, and mercury solutions (after Westwood et al. [20]).

showed that an additional increment of strain was always required to cause fracture in a Cu–8 wt% Al alloy after wetting with mercury. This result suggests that freshly-deformed solid surface must be exposed in the presence of the liquid metal before embrittlement will occur, but the process is obviously complex because the additional strain needed decreased with increasing strain before contact.

The need for good wetting has occasionally led to some confusion in the identification of embrittling combinations because wetting has been correlated with solid/liquid reaction or extensive mutual solid solubility [22,23]. In practice, LME is usually associated with the absence of these factors, thus leading to an apparent conflict. The difficulty has been resolved to some extent by more recent work using UHV techniques or ion-bombardment to remove surface oxide films. For example, excellent wetting has been induced in couples such as Na/Fe, Na/Ni, Hg/Fe and Hg/Ni, none of which shows either interaction or mutual solubility [24,25]. This result could be predicted from the surface and interfacial energies [26] and, indeed, low melting-point metals might be expected to wet most solid metals, and especially the transition metals. This implies that much of the difficulty encountered in achieving good wetting, and hence some of the uncertainty in identifying couples susceptible to LME, can be attributed to contamination by surface films.

Good solid/liquid contact is necessary for crack propagation as well as nucleation. If the supply of the liquid embrittler to the crack-tip is interrupted, for example by freezing, then the fast fracture is arrested [18,27]. However, Stoloff has also pointed out that if the solid is notch-sensitive, then fracture could occur in the absence of a continuous supply of the embrittler if the crack exceeds the critical size [28].

2.3. Temperature dependence

In many susceptible systems embrittlement is restricted to a sharply-defined temperature range. The onset invariably occurs near the melting point, T_m, of the embrittler, in keeping with the observation above that the liquid metal must follow the crack-tip for propagation to continue. In a few cases, however, the embrittlement extends to temperatures below T_m. For example, an AISI 4140 steel is embrittled by

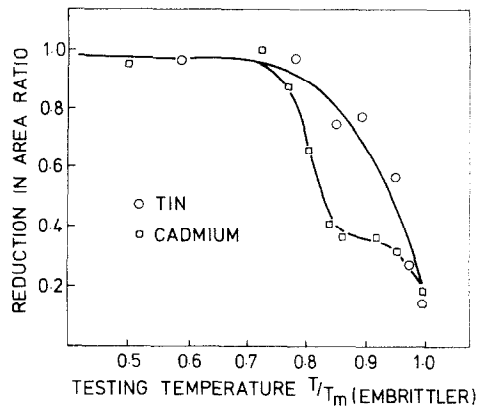

Fig. 2. Embrittlement of an AISI 4140 steel by solid metals (after Lynn et al. [29]).

cadmium, indium, lead, tin and zinc from $0.75T_m$ [29] (fig. 2). The high vapour-pressure metals are presumably transported through the vapour phase, but for those with low vapour pressure (e.g. tin and indium), some other mechanism such as surface diffusion must be invoked. Other studies on titanium alloys [30,31] and steels [32,33] have shown that cadmium in particular can cause sub-critical crack growth in statically-loaded specimens at temperatures as low as 40°C.

Embrittlement at unexpectedly low temperatures may also occur if a low melting-point eutectic is formed. Thus zinc is embrittled by tin (T_m = 232°C) down to 198°C [34]. This observation complements earlier findings that some solids are embrittled by contact with metals of higher melting point when a eutectic occurs [35]. Thus pure tin is embrittled by zinc, lead and magnesium in the temperature interval between its melting point and the respective eutectic temperature (table 1).

As the temperature is increased through the embrittlement range, a sharp return of ductility is

Table 1
Embrittlement of tin (T_m = 232°C) by higher melting-point metals

	T_m (°C)	Eutectic temperature (°C)
Zinc	419	198
Lead	327	183
Magnesium	650	200

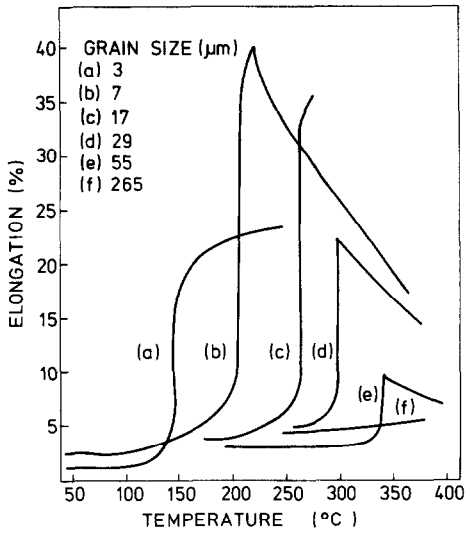

Fig. 3. Dependence of the transition-temperature of α-brass in mercury on grain-size (after Rostoker et al.)

often observed, giving a brittle-ductile transition similar to that in some steels and other bcc and hcp pure metals. The analogy is extended by dependence of the transition on the grain size of the solid (fig. 3) or the strain-rate (fig. 4). The lower temperature for the onset of LME is usually independent of strain rate, so that the width of the embrittlement range is altered. Fig. 5 demonstrates this behaviour in zinc embrittled by indium [34]; the narrowness of the range at the lowest strain-rate (12°C) illustrates the practical difficulty of ensuring detection of any possible embrittlement.

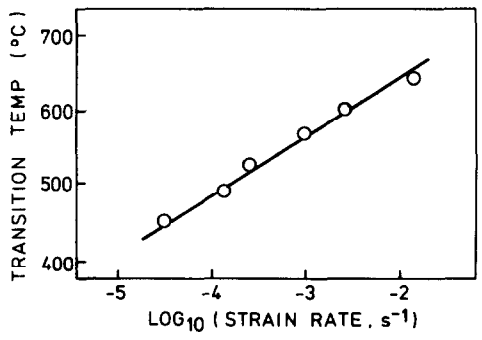

Fig. 4. Dependence of the transition-temperature of titanium in cadmium on strain-rate (after Robertson [62]).

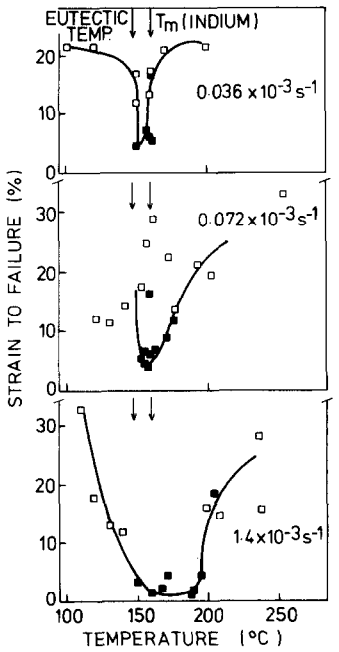

Fig. 5. Dependence of embrittlement temperature range of zinc in indium on strain-rate (after Old and Trevena [34]).

2.4. Compositional effects

Changes in composition of both solid and liquid can alter the severity of embrittlement even to the extent of promoting it where it was previously absent or vice versa. Normally, such effects require significant changes in composition at the percent level and it is unusual to find that ppm quantities of impurities are important. For example, failure strains of copper–aluminium alloys in mercury fall progressively from 40 to 5% as the aluminium content rises from 6 to 16% [36]. Conversely, additions up to 60 a/o of indium to mercury increase the embrittlement of cadmium but have the opposite effect on silver [37].

Although most of the changes are comparatively slow, some additions are more potent. Embrittlement of AISI 4145 steel by lead is increased by additions of up to 9% of tin, but a similar effect is produced by only 2% of antimony [38]. Additions of zinc are stated to be even more effective [39]. Several other examples are known where the addition of an element, frequently of higher melting point, is more embrittling in solution at lower temperatures than it

is in its pure state at higher temperatures. Thus although Rostoker et al. reported that some aluminium alloys were not embrittled by pure cadmium at 380°C [15], fig. 1 shows that quite small additions of cadmium to mercury are effective at room temperature. Kamdar has suggested that this "inert carrier" approach might be useful for studying LME by higher melting-point metals [40].

2.5. Metallurgical condition

LME also depends sensitively upon the thermal and mechanical history of the solid. Rosenberg and Cadoff [41] found that the proportionate reduction in ductility of pure copper in mercury rose from less than 20 to about 35% as the grain size increased from 0.113 to 0.485 mm. Furthermore, if testing is carried out at a single temperature, then the apparent presence or absence of embrittlement depends upon grain size.

Alloys in high-strength conditions are usually more severely embrittled [42]. Nichols and Rostoker have shown that solution-hardening in an Al 2024 alloy led to more severe embrittlement by mercury, although fracture always occurred after macroscopic yielding [19]. In contrast, precipitation-hardened alloys broke at only 70% of the unwetted yield stress. Maximum embrittlement coincided with the existence of coherent precipitates, and was alleviated by overageing. The combination of strain and heat-treatment was particularly detrimental and precipitation-hardened specimens pre-strained 20% failed at only one fifth of the unwetted yield stress; again, further deformation alleviated the embrittlement. Somewhat similar effects were also observed in an Al–4.5 wt% Mg alloy, where plastic prestrains of around 5% caused maximum embrittlement, but in this case the variation was attributed to strain-ageing caused by the rapid redistribution of the magnesium atoms [43]. In some systems, however, increasing deformation is beneficial, as shown by Breyer and Watkins, who found that embrittlement of AISI 4145 steel by both internal lead and an external Pb–4 wt% Sn alloy was almost completely eliminated by a reduction of 50% [44].

In addition to general microstructure, the grain-boundary chemistry is also important, as might be expected in a process which can involve intergranular fracture. However, in contrast to temper embrittlement, where segregation to grain-boundaries is always accompanied by increased brittleness, the effect on LME is more variable. Thus although segregation of tin and antimony exacerbated the embrittlement of a doped AISI 3340 steel by lead [45], arsenic had little effect and phosphorus was slightly beneficial. Phosphorus was also particularly beneficial in copper–nickel alloys, where a heat-treatment which might have been expected to cause segregation completely suppressed embrittlement by mercury [46]. It is also possible that segregation contributes to the influence of grain-size on LME, since a given solute content will give higher grain-boundary concentrations at larger grain-sizes.

2.6. Fatigue

Most LME data relate to short-term tests in bending or uniaxial tension and only a few isolated papers consider longer-term performance. However, it is clear that combinations which are susceptible at higher strain rates (e.g. 10^{-3}/s) can also show embrittlement at lower stresses, both cyclic and static. Rostoker et al. [15] state that unspecified aluminium alloys loaded to half the yield stress in mercury at 100°C fail in tens of minutes. Cyclic fatigue loads are reduced to about 40% of the loads in air for the same life. Slightly different behaviour was noted for an AISI 4340 steel in mercury, where degradation was found only in the low-stress, high cycle range. Little information exists on the effects of cyclic loading below the embrittler melting point, but there are indications that this combination will also cause failure [47,48]. In general, there is no evidence that fatigue conditions are more severe than monotonic loading, although in one study, a cold-worked aluminium–bronze was found to be embrittled by mercury in tensile fatigue but not in simple tension [49].

2.7. Susceptibility to LME

The previous sections have not attempted to provide comprehensive information on all the reported observations of LME, but rather to establish trends of behaviour. These demonstrate that both the occurrence and severity of LME are sensitive to test-

ing conditions and metallurgical variables. It is therefore difficult to identify susceptible systems with certainty, especially since small but important changes in conditions or composition have sometimes been overlooked in reviews of available data. As a result, a general view has become established that LME is a specific property of closely defined materials in particular circumstances and at least three early reviews have accepted this specificity as a fundamental characteristic [15,28,40]. In the light of more recent data, however, Shunk and Warke have suggested that this concept is without theoretical foundation [50] and, over fifteen years ago, Rosenberg and Cadoff commented that discrepancies in results probably indicated the complexity of the problem rather than the contradiction of observations [41].

In view of this uncertain background, it is not surprising to find that attempts to predict the occurrence of LME are largely empirical. Thus it has been noted [40] that susceptible systems tend to show

(a) limited mutual solid solubility,

(b) no tendency to form intermetallic compounds,

(c) similar Pauling electronegativities.

Although these statements apply in many cases, it must be emphasised that they are correlations and not explanations. Furthermore, there are many exceptions. Aluminium is embrittled by gallium, and both tin and zinc will embrittle some steels, despite solid solubilities of several percent. Also, the Fe/Sn, Fe/Zn and Ti/Cd systems show intermetallic compounds as well as LME. The electronegativity rule is similarly unreliable; aluminium (Pauling electronegativity 1.5) is reported to be embrittled by sodium (0.9) and iron (1.8) by lithium (1.0), despite differences in their electronegativities.

Apart from the difficulties in predicting the behaviour of individual systems, perhaps the most noticeable shortcoming of the empirical correlations is that they are based entirely on chemical identities and take no account of testing and metallurgical parameters. Many authors [40,51,52] have commented that, in view of the well-established influence of these factors, a better understanding is required to support liquid-metal technology. Until such an understanding is reached, information on particular systems given in broad digests should always be supplemented by reference to original papers.

3. The mechanism of LME

3.1. Suggested mechanisms

Proposed mechanisms for LME include stress-assisted dissolution [53], air pressure in pre-existing cracks [54], the formation of a weakly-bonded alloy zone ahead of the crack-tip [55,56], easier nucleation and movement of dislocations [57,58] and adsorption-induced reductions in surface energy [15,59,60], strength [61], bond-strength [27,52], or cohesion [40]. The stress-assisted dissolution model was subsequently retracted because it predicted more severe embrittlement at higher temperatures [62], whereas the opposite is often found in practice. The theories of the Russian workers on the formation of brittle alloys near the crack-tip have not yet been fully investigated, but high crack velocities suggest that any process involving a diffusion step is unlikely [63,64]. Similarly, Lynch's proposal of easier dislocation nucleation and movement is attractive in some respects, but has yet to account for the general features of LME in polycrystalline materials.

In the light of present knowledge, an adsorption-induced reduction in strenth would appear to be most likely, but the detailed mechanism has yet to be elucidated. For example, Kamdar draws a sharp distinction between reduction in cohesion and surface energy [40], and Oriani and Josephic take a similar approach in the related field of hydrogen embrittlement [65]. There is thus some confusion as to the definition and relationship of cohesion, mechanical strength, bond-strength and surface energy, and the role of metallurgical parameters. In an attempt to reach a broader understanding, several workers have considered the reduction in bond-strength models in terms of the Cottrell–Petch approach to the brittle/ductile fracture of iron and steels [66,67]. This model involves both plastic yield and surface energy and hence incorporates both metallurgical and environmental factors. In particular, the brittle/ductile transitions observed in LME are closely similar to those found in some steels, bcc and hcp metals, and have been analysed in an analogous manner [62, 68].

The only major objection to this approach was lodged by Preece and Westwood, who argued that the original theory was formulated for brittle fracture at

a well-defined yield point in iron, whereas fracture during LME can occur before or after general yield [69]. It was therefore proposed that the return of ductility was due to the thermal desorption of the liquid embrittler from the solid surface. However, the mechanism of the desorption from a surface which remains covered by a bulk liquid phase was not described in detail, and remains difficult to envisage. Furthermore, the theory of brittle fracture suggests that failure occurs when a crack nucleus is subjected to some critical stress and there is no a priori reason why work-hardening with further plastic strain should not provide a means of reaching that stress. The yield stress itself is therefore of limited significance. At present, therefore, the Cottrell–Petch view of competition between elastic fracture and plastic deformation still seems preferable.

3.2. The theory of brittle fracture

This section outlines very briefly the main results of the theory of brittle fracture for comparison with LME. In most cases, the results are stated without proof.

The role of the surface energy γ in determining the tensile fracture stress σ_G of an elastic solid was first elucidated by Griffith [70]. Equating the reduction in strain energy to the increase in surface energy needed to propagate a crack of length c under plane strain, gives

$$\sigma_G = (2E\gamma/\pi c(1-\nu^2))^{1/2} , \quad (1)$$

where E is Young's modulus and ν is Poisson's ratio. Since E, ν and γ are substantially independent of temperature, so also is the fracture stress.

When this theory was extended to metals it was found that the crack lengths necessary to explain the measured brittle fracture strengths were of the order of micrometres. Such cracks were not always present before testing, and it was therefore proposed that they could be nucleated by the coalescence of dislocations against an obstacle such as a grain boundary. In 1957, Stroh [71] showed that the condition for fracture by this mechanism when n dislocations of Burgers vector b were piled up against a barrier by a shear stress on the slip plane was

$$\sigma_S nb = 12\gamma . \quad (2)$$

An alternative model, due to Cottrell [67], considers the propagation of a crack nucleus formed by coalescence of dislocations on the {110} planes of a bcc lattice. Fracture occurs under a tensile stress σ_C when

$$\sigma_C nb = 2\gamma . \quad (3)$$

Although eq. (2) and (3) are similar, the stresses are different because Stroh considered the stress acting on the slip plane whereas Cottrell's model refers to an external applied stress.

The number of dislocations, nb, which will pile-up under a given stress was calculated by Eshelby et al. [72]. When fracture occurs after yielding, this number is constant at approximately

$$nb = (\sigma_y - \sigma_i)\, d/\mu , \quad (4)$$

where σ_y is the yield stress, σ_i the friction stress, d the grain size and μ the shear modulus. Since the yield stress is related to the grain size by an experimental constant, k_y, so that

$$\sigma_y = \sigma_i + k_y d^{-1/2} , \quad (5)$$

then from eq. (3)

$$\sigma_C k_y d^{1/2} = \beta\mu\gamma , \quad (6)$$

where β is a constant. Eq. (2), (3) and (6) relate fracture stress to surface energy, and thus an environment which lowers the surface energy of a particular solid will also tend to embrittle it.

This view has been questioned because the thermodynamic surface energies of metals are about 1–2 J/m^2, whereas the measured specific fracture energies from mechanical tests are usually at least an order of magnitude higher. The increase is attributed to the plastic deformation which occurs at the crack-tip during fracture. It has therefore been stated that reductions in thermodynamic surface energy are small in comparison with the total fracture energy and hence cannot have a major effect on mechanical strength. However, this view is countered with the argument that the plastic contribution depends upon the tensile bonding between atoms at the crack-tip, which in turn is a measure of the thermodynamic surface energy. If, therefore, the thermodynamic surface energy is reduced, then the maximum stress at the crack tip is reduced, and consequently the plastic strain and the fracture surface energy will be reduced

in proportion. In the limit, zero thermodynamic surface energy leads to zero stress at the crack tip and hence zero fracture energy.

The brittle/ductile transition in α-Fe and ferritic steels has been consiered in detail by Stroh and Petch. In contrast to the brittle-fracture strengths, the yield strengths of bcc metals fall rapidly with increasing temperature and both authors base their theories on this fact, although from slightly different aspects. Stroh calcualted a transition temperature for the recovery of ductility, T_R, by considering the probability of nucleation of a dislocation (i.e., plastic flow) at a crack tip during deformation of a metal at a strain rate $\dot{\epsilon}$ to obtain

$$\frac{1}{T_R} = -\frac{k}{U}\ln \dot{\epsilon} - \frac{k}{U}\ln d^{1/2} + C\gamma^{1/2}, \qquad (7)$$

where k is Boltzmann's constant, U is stress-dependent activation energy and C is a material constant. A slightly different approach by Petch calculated the temperature at which the yield stress, which was assumed to decrease exponentially with increasing temperature, fell below the brittle fracture stress, giving

$$\beta' T_R = \ln B - \ln\left(\frac{4q\mu\gamma}{K'} - K'\right) + \tfrac{1}{2}\ln d, \qquad (8)$$

where β' and B are materials constants, q is a stress concentration factor, and K' and experimental constant.

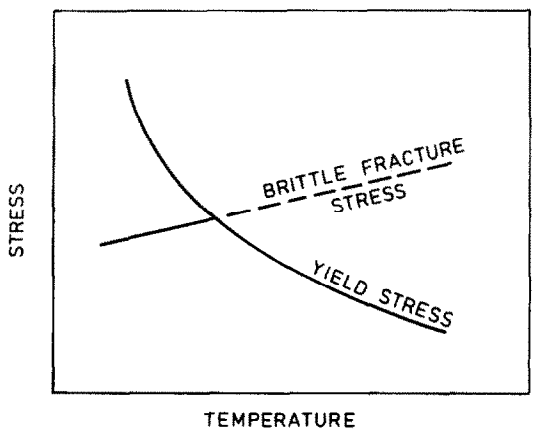

Fig. 6. Temperature dependence of yield and brittle fracture stresses in bcc metals (schematic).

Although they differ in detail, both models predict an increase in T_R with larger grain-size and smaller surface energy and also Stroh's model predicts higher T_R with higher strain rate. In addition fig. 6 suggests that increases in yield stress should also raise T_R.

3.3. LME as a brittle fracture process

To help assess the influence of nuclear applications on LME, it is useful to consider first the validity of the theory outlined above.

There is good evidence for a nucleation strain in LME. In the few isolated instances where fracture takes place at very low strains, e.g. ~1%, local microplasticity is presumably responsible. Clear evidence of separate nucleation and propagation stages can be seen in the embrittlement of an AISI 4140 steel by zinc over a temperature range spanning the zinc melting point (260–422°C) [29]. At lower temperatures, many cracks were nucleated but propagation was slow, probably because the transport of the zinc to the crack-tip was limited to vapour or surface diffusion. As the temperature increased, progressively fewer cracks were formed until, above the melting point (419°C), only one crack was nucleated and propagated catastrophically in the presence of the liquid metal. Similar behaviour occurred with lead, cadmium, tin and indium. A further and unequivocal demonstration of nucleation was reported by Kamdar and Westwood [16]. When zinc single crystals were carefully handled so as to avoid the creation of barriers to plastic flow by mechanical damage, then embrittlement by mercury was completely suppressed.

Brittle/ductile transitions in LME also provide strong links with the Cottrell–Petch model. It is interesting to note, however, that intrinsic brittle/ductile behaviour is limited primarily to bcc and some hexagonal metals. In contrast, LME transitions also occur in fcc metals [69]. Since yield stresses vary more quickly with temperature in bcc than in fcc metals, it would be informative to compare the transitions in samples of the two structures.

The theory also suggests that lower ductility during LME should be associated with increasing transition temperature, since the embrittlers with lower interfacial energies on the solid metal will delay the intersection of brittle failure and yield stress

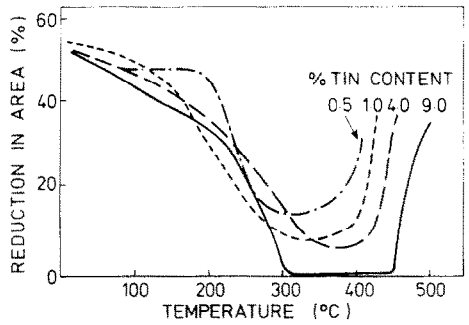

Fig. 7. Embrittlement of AISI 4145 steel by lead–tin alloys (after Breyer and Johnson [38]).

curves until higher temperatures (fig. 6). Evidence for this is sparse because a wide temperature interval of embrittlement and a sharp transition are required to establish the correspondence and there are only a few results on suitable systems. Nevertheless, the trend is clearly visible in work on the embrittlement of steels by lead alloys and copper–bismuth alloys by mercury [38,73] (fig. 7). Further analogies are provided by the effect of grain size on transition temperature, although occasional exceptions are known [68].

The influence of yield stress is also generally in accord with the brittle fracture model. All increases appear to worsen the embrittlement, irrespective of whether they arise from precipitation hardening [19], solution hardening [36,41], or quenched-in defects [74]. The raising of the maximum principal stress for yielding at a notch root is also detrimental [2]. The effects of strain-rate are less well-proven, but increasing rates have been shown to reduce ductility or increase transition temperatures during LME of several metals [15,34,62,68].

Although the effects of alloying have been attributed solely to increases in yield stress [41], Stoloff and his co-workers have identified additional factors [36] in LME which have not been investigated for intrinsic brittle fracture. Solute additions to pure iron [75] and pure copper [73,76] increase the yield stress dependence on grain size, k_y, and also increase the concentration and planarity of the slip bands. It was suggested that the increase in k_y will lead to a lower fracture stress through eq. (6), but McLean has also commented that planar slip is more likely to nucleate brittle fracture than diffuse slip [77]. It is therefore difficult to separate the effects of alloying on yield stress and deformation behaviour.

3.4. The prediction of LME

While the qualitative effects of metallurgical and testing parameters are reasonably clear, there is no similar understanding of the chemical factors which produce LME in one combination and not in another. Several authors have attempted to predict reductions in bond strengths by a variety of routes. The three empirical correlations noted in section 2.7 provide general support for this approach because they all indicate weak interatomic bonding. Chaevski [55] and Chaevski and Popovich [56] suggested the formation of a weakly-bonded metastable solid solution at the crack-tip whose strength could be related to a positive deviation from Raoultian solution behaviour and hence to positive heats of mixing in the liquid–solid couple. Similar calculations by Kelley and Stoloff [52] used an Engel–Brewer technique.

A more direct link between chemical interaction and brittle fracture follows a suggestion by Klein-Wassink [23]. For many pure elements there is good agreement between the surface energies and bond strengths as indicated by melting points or heats of vaporisation [78,79]. It was therefore proposed that, by analogy, interfacial energies might be estimated from heats of mixing. This link was explored by Tetelman and Kunz [80], who applied the argument to hydrogen embrittlement, liquid metal embrittlement, and temper embrittlement, but comparison was hampered by a lack of reliable data. The most recent attempt in this direction [81] uses heats of mixing estimated from a semi-empirical model by Miedema and Den Broeder [82]. According to this approach, low positive values imply low interfacial energies which in turn indicate low fracture stresses and hence embrittlement. High values imply only weak or absent embrittlement while negative values indicate chemical reaction. Thus the data in table 2 identify zinc and cadmium as potential embrittlers of aluminium, and accord with the results in fig. 1. Similarly, the data are consistent with experimental observations of LME of ferrous alloys by cadmium, mercury, indium, copper, lead, tin and zinc. The alkali metals lithium and sodium are seen to have different effects on copper and iron. Cu/Li is identified as a reactive

Table 2
Calculated average partial heats of mixing (kJ/g · atom) for solid–liquid couples (after Miedema and Den Broeder [82])

Liquid	Bi	Cd	Cs	Cu	Ga	Hg	In	Li	Na	Pb	Sb	Sn	Zn
Solid													
Al	40	13	112		4	15	27	−14	52	41		16	2
Cu	21	−4	89		−29	5	1	−39	37	25		−10	−20
Fe	113	64	370	59	−7	90	79	95	236	126	45	45	15

system, whereas copper is embrittled by sodium. In contrast, lithium is more likely to embrittle ferrous alloys because its heat of mixing is similar to that of other embrittlers, but the lack of LME by sodium is presumably due to its high heat of mixing.

In summary, then, there is reasonably convincing evidence for interpreting LME as a form of environmentally assisted elastic fracture. Most of the experimental data can be qualitatively explained within such a framework, although recent observations of ductile dimple fracture [57,58] are apparently in conflict and there is still a need for more quantitative data on the chemical aspects. It is against this background that the next section gives a broad survey of radiation effects and attempts to identify those which might interact synergistically with LME.

4. Radiation effects and their implications for LME

Several different kinds of radiation are encountered in fission and fusion reactors, but from the discussion in the previous sections, it is clear that only those radiations which alter mechanical properties or cause significant changes in composition by transmutation will be relevant to LME. This criterion eliminates β and γ radiations since their contributions to displacement damage and transmutation are small, particularly in comparison with neutron damage. Ionization is unimportant in metals because of electron mobility. If attention is confined to the neutron flux, then only the core of the reactor need be considered, i.e. the primary support and containment structure and fuel cladding in the fission reactor and first wall and blanket components in the fusion reactor.

In addition to the displacement damage and transmutation caused by neutrons, cladding alloys in particular are subject to similar effects from the fission process itself. Each fission produces two energetic fragments, some of which reach the internal wall of the fuel can. Also, the accumulation of metallic and non-metallic fission products escaping from the fuel might produce an embrittling environment at the inner wall of the stressed cladding.

4.1. Displacement damage

Neutron energies in nuclear reactors vary from 14.1 MeV (fast neutrons) produced by the D-T fusion reactor, through thermal energies ~0.1 eV (thermal neutrons) down to $\sim 10^{-2}$ eV (cold neutrons). Fast neutrons therefore possess sufficient energy to displace many matrix atoms in a series of widely spaced collisions. Each matrix atom struck by the neutron (the primary knock-on atom) acquires on average enough kinetic energy to displace a number of its neighbours and give rise to a cascade of closely spaced collisions leaving a cluster of vacancies and throwing off atoms into interstitial sites. Although some of these point defects are mutually annihilated almost immediately, the vacancy-rich core of the cascade may collapse to form a stable dislocation loop surrounded by a shell of mobile interstitials which are lost at sinks or may form clusters. Elementary models of radiation damage suggest that a 2 MeV neutron in α-Fe will displace about 1400 atoms [83]. The saturation concentration of vacancy–interstitial (Frenkel) pairs is estimated at $\sim 10^{-3}$ for Al, Cu, Ag and Au at very low temperatures, i.e. <20 K, in a high-flux reactor [84]. This is about two orders of magnitude greater than the thermal equilibrium vacancy concentration of a metal near its melting point [85].

Fission fragments also displace atoms but there are important differences from neutron damage. The

Table 3
Collision characteristics of neutrons and fission fragments with atoms of mass 50 [84]

Particle	Distance between primary collisions	Particle track length
100 MeV fission fragment	1 nm	1 μm
2 MeV neutron	50 mm	0.1 m

fragments are peaked around mass 96 and energy 95 MeV, and mass 139 and energy 55 MeV [84]. The collision cross-sections of such particles are very large, and the fragment is therefore rapidly arrested. Fission fragment damage is thus concentrated in the fuel and inner wall of the cladding (table 3).

The influence of displacement damage on materials properties depends upon the energy spectrum, total dose, and irradiation and test temperatures. The spectrum and dose control the amount of damage sustained, while the temperature governs its redistribution and final form. In addition, the effect on properties during irradiation (in-pile) differs from the effect after removal from the reactor (post-irradiation).

4.1.1. In-pile effects

Different mechanisms for the condensation of vacancies and interstitials can produce dimensional instabilities. If these instabilities are restrained within an engineering structure, stresses could be set up which might contribute to failure by LME. It is therefore necessary to estimate first of all the size of the radiation-induced strains. Two processes are of interest, radiation growth and void-swelling.

(a) Radiation growth

In isotropic materials at low temperatures, the effects of vacancies and interstitials almost counterbalance and dimensional changes are therefore small. In anisotropic materials, however, significant growth can occur. It has been postulated that this arises because the unequal thermal expansion coefficients cause the vacancies and interstitials to favour different condensation sites during the quench of the displacement spike [86]. In zirconium alloys, for example, vacancy clusters collapse into loops with Burgers vectors which have a large component parallel to the *c*-axis. Atoms are thus transferred from basal to prism planes, with a resultant change in shape at essentially constant volume [87].

Radiation growth is marked under fission fragment bombardment, where α-uranium, being both fissile and orthorhombic, shows changes in dimensions of up to 1000%. Smaller effects occur in other anisotropic metals including cadmium, zirconium, zinc and titanium. Magnesium has isotropic thermal expansion coefficients and therefore does not grow. Some cold-worked cubic materials can also show radiation growth, presumably due to condensation of point-defects on anisotropic dislocation structures [88]. Foils of pure copper, iron, gold, nickel and aluminium showed strains of 2×10^{-3} after irradiation to 10^{17} fission fragments per cm^3 at 0.25–0.3 T_m.

Although radiation growth is greatest under fission fragment bombardment, anisotropic materials will also grow under neutron irradiation and there are many reports in the literature on the behaviour of zirconium alloys because of their use in water reactors [89]. Growth is texture-dependent and increases with dose in cold-worked material, whereas there is evidence of saturation in annealed material. Strains up to 3×10^{-3} have been measured after irradiation to 10^{22} n/cm² at 340°C, and Harbottle and Cornell estimate a total strain of 9×10^{-3} in cold-worked Zircaloy after a life dose of 2×10^{22} n/cm² [90]. Radiation-growth strains in anisotropic constructional materials can thus approach 1%.

(b) Void-swelling

Although cubic materials, even when cold-worked, do not exhibit constant-volume growth under neutron irradiation, some alloys suffer from void-swelling at high doses. This is due to an imbalance in the rate of absorption of vacancies and interstitials at the different sinks in the crystal, leading to an excess of vacancies at 0.3–0.5 T_m (approximately 450–750°C in austenitic steels [91]). The resultant swelling varies with irradiation parameters, composition and microstructure, but can amount to several percent in AISI 316.

Void-swelling is particularly marked under intense fast neutron irradiation such as in the LMFBR core, where total doses approaching 100 displacements per atom (dpa) are expected at operating temperatures in the void-swelling range. Furthermore, because of gradients in temperature and neutron flux within the

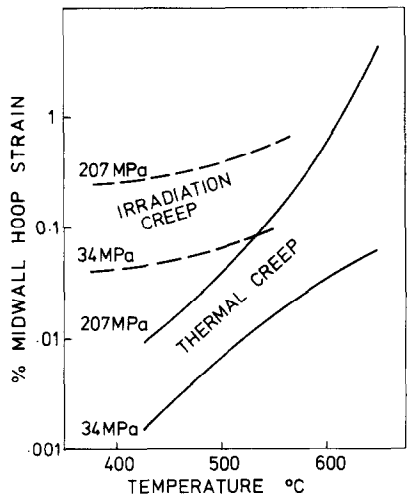

Fig. 8. Irradiation and thermal creep regimes in 20% cold-worked AISI 316 (after Gilbert et al. [95]).

core, the swelling is non-uniform and causes distortion of the fuel assemblies. This may be counteracted either by rotating the assemblies periodically or physically restraining the distortion by clamping.

There are thus two mechanisms by which radiation can induce strain, but fortunately the effects are mitigated by irradiation creep. In unirradiated materials, creep is usually insignificant below 0.5 T_m, but the point defects created by fast neutron irradiation cna contribute to creep processes at lower temperatures, although the exact mechanisms are still a matter of discussion [92]. Creep rates are therefore increased at temperatures where thermal creep is inoperative [92,93]. For example, Watkins and Wood [94] found that the secondary creep-rate of Zircaloy-2 was increased by an order of magnitude at 300°C in a flux of 2.4×10^{13} n/cm^2 · s. Similar increases have also been measured in cold-worked AISI 316 using pressurised tubes in EBR-II [95] (fig. 8). As well as increasing low-temperature creep rates, irradiation can enhance overall creep ductility. Cold-worked zirconium alloys reach 10% strain at creep rates $<10^{-5}$/h [89] under irradiation whereas tertiary creep begins after only 1–3% strain in out-of-pile tests.

In trying to estimate the stresses set up by radiation growth and void-swelling in competition with radiation creep, the important parameter is strain-rate rather than strain, because it is the former which governs the creep stress. Radiation growth data for Zircaloys indicate that the highest strain-rates occur at low doses. This is marked in annealed material [96]. Assuming that the initial growth in linear, experiments by Murgatroyd and Rodgerson suggest a strain-rate of 0.5×10^{-9}/s over the first 10^6 s. Northwood and Fidleris quote similar results for both annealed and cold-worked samples [87,89]. The stress necessary to accommodate these strain-rates by creep can be estimated from the empirical equation derived by Watkins and Wood for internally pressurised tubes of Zircaloy-2 [94]

$$\dot{\epsilon} = 1.1 \times 10^{-20} \exp\left(\frac{-14000}{RT}\right) \phi^{0.85} \sinh(0.0167\sigma) , \quad (9)$$

where $\dot{\epsilon}$ is the strain rate in s^{-1}, ϕ is the fast neutron flux in $m^{-2}s^{-1}$ and σ is the stress in MPa. At 300°C, eq. (9) gives a stress of about 140 MPa. This is 50% greater than the nominal hoop stress quoted for the Winfrith SGHWR (84.5 MPa), or about half the yield stress at temperature [97].

It is unlikely that much greater stresses will arise because the strain-rate increases very rapidly with increasing stress. Below 50 MPa, $\sinh(0.0167\sigma) \sim 0.0167\sigma$ and thus $\dot{\epsilon}$ depends linearly on σ. At higher stresses, however, the exponent increases from 2–3 at 200–400 MPa to about 100 at 600 MPa. Stresses significantly above the yield stress are therefore unlikely to be generated by any growth-rate which could reasonably be foreseen in practice.

There are insufficient data on void-swelling to assess analytically the stresses arising in a restrained component, but computer modelling studies of the restrained core in the proposed CDFR indicate that axial tensile stresses in the fuel-element wrappers will not exceed 30 MPa [98]. Hence neither void-swelling nor radiation growth are expected to lead to stresses approaching the yield stress. Data from systems known to be susceptible to LME show that embrittlement is rarely initiated at such stress levels, although isolated examples are recorded.

4.1.2. Post-irradiation properties

At moderate temperatures, a significant fraction of the interstitial defects agglomerate into clusters up to a few tens of nanometers in diameter, while the

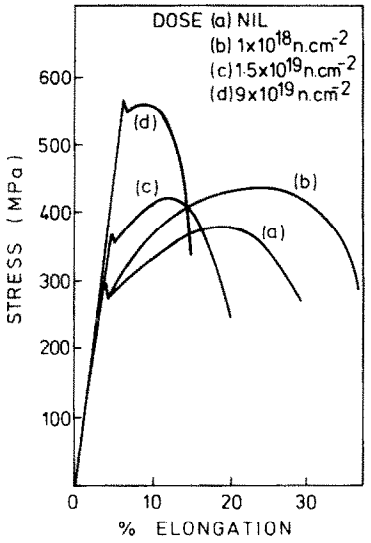

Fig. 9. Hardening of carbon steel by irradiation with thermal neutrons (after Makin et al. [99]).

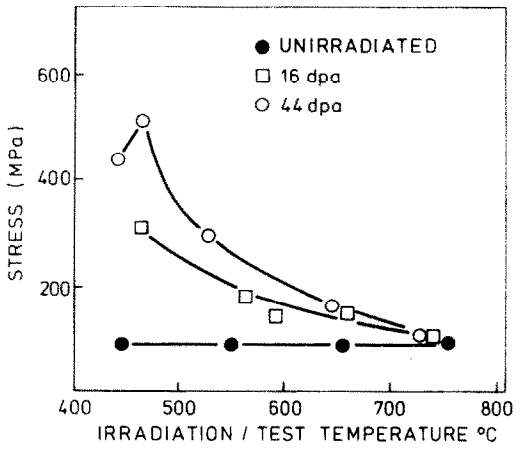

Fig. 10. Irradiation hardening of the yield stress of annealed AISI 316 by fast neutrons (quoted by Harries [106]).

vacancy clusters remain in situ at the sites of the collision cascades. The resulting distribution of interstitial loops obstructs dislocation movement and causes irradiation hardening in many metals. Post-irradiation properties are therefore altered in the opposite direction to in-pile creep properties.

Hardening increases progressively with irradiation (fig. 9). Experiments at different grain sizes show that the yield stress σ_y is proportional to $(\text{dose})^{1/3}$, but k_y remains constant. The major part of the hardening has therefore been attributed to increases in σ_i, similar to precipitation hardening [99]. In accord with the model of brittle/ductile fracture described in section 3.2., the increase in yield strength raises the transition temperature of iron and ferritic steels. Nichols and Harries quote increases of 80°C in ferritic pressure vessel steels for doses of 6×10^{18} n/cm^2 > 1 MeV [100]. Wullaert et al. obtained good agreement between measured and calculated effects of the increased yield strength on brittle/ductile transition temperatures [101].

Information on austenitic alloys, including AISI 316, AISI 304 and Inconel 718 has been generated from programmes on fast reactor materials [102–105]. Harries has collated results for both annealed and 20% cold-worked AISI 316 irradiated and tested at similar temperatures in the range 400–800°C [106]. Up to about 480°C, the yield stress of annealed materials increases by as much as a factor of five, but falls off steadily as the temperature increases (fig. 10). Ductilities are initially much reduced, but recover in the middle of the temperature range. In contrast to the normal pattern of radiation-hardening, heavily cold-worked material can show some softening because the high concentration of radiation-induced defects can contribute to annealing. At moderate temperatures, therefore, the ductility is increased (fig. 11).

Studies of post-irradiation creep and rupture

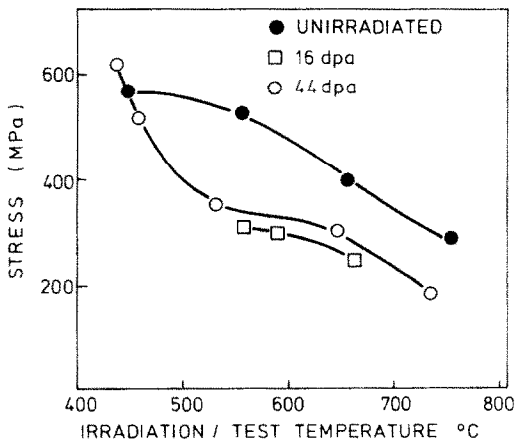

Fig. 11. Irradiation softening of the yield stress of 20% cold-worked AISI 316 by fast neutrons (quoted by Harries [106]).

behaviour are not directly applicable to LME, but may be useful as an indication of resistance to the slow propagation of brittle cracks. High creep-rates and creep ductility will favour crack blunting rather than brittle failure, although the temperature range for creep, say >500°C in the case of austenitic alloys, is near the top of the range of interest for LME. Nevertheless, it is worth noting that the creep rate, rupture life, and ductility of annealed AISI 316 at 540 and 650°C, are reduced after irradiation [106]. The behaviour of 20% cold-worked material is more complex. Up to 650°C, irradiation has an adverse effect on creep properties, but at higher temperatures some improvement occurs due to irradiation-assisted recovery and partial recrystallisation. The effects on creep behaviour are thus similar to the effects on short-term properties.

Data for irradiation under fusion conditions are limited. The major difference from fission conditions is the high energy (14.1 MeV) of the neutrons from the fusion reaction. Preliminary investigations suggest that the displacement damage can be calculated with reasonable accuracy. Experiments in the High Flux Isotope Reactor with annealed and 20% cold-worked AISI 316 [107] indicate that the yield stresses in both conditions are lower than after the same dose in fast reactors. This is likely to be beneficial from the point of view of LME, but is offset by high concentrations of transmutation helium at the grain-boundaries which lower the ductility to near zero above 650°C.

In addition to the changes in bulk mechanical properties, fast neutron irradiation also gives rise to important differences in microstructural deformation

Fig. 12. Slip-steps at emergent dislocation channels in neutron-irradiated pure copper (courtesy Sharp [109]).

and fracture behaviour. It was noted earlier that at moderately low temperatures, e.g. $\leqslant 0.35\ T_m$ for austenitic alloys, a uniform distribution of fine defect clusters was produced. Transmission microscopy shows that during subsequent deformation, the first dislocations released sweep clear channels 0.1–0.2 μm wide along the glide-plane. Because of the removal of the damage in these regions, further deformation preferentially follows the same track, giving intense localised shear, known as dislocation channelling. This phenomenon occurs in many pure metals and alloys, including iron, ferritic [83] and austenitic steels [106]. Microscopic examination of deformed specimens also shows marked slip-band coarsening [108] with consequently larger slip steps produced at the surface. Experiments by Sharp [109] on irradiated copper single crystals established the correspondence between these steps and emergent dislocation channels (fig. 12).

There is a strong resemblance between dislocation channelling and the slip-band coarsening which is associated with increased liquid metal embrittlement [36,75]. If crack nucleation takes place by a pile-up mechanism as described in section 3.2, then slip coarsening by either irradiation or alloying might of itself increase susceptibility to LME. This is in accord with the comment of Makin et al. [99] that the effects of irradiation on mechanical properties are in some respects similar to those of alloying.

4.2. *Transmutation*

Transmutation occurs by both neutron capture in non-fissile elements and also by fission of heavy atoms within the fuel.

4.2.1. *Transmutation in non-fissile elements*

Both fast and thermal neutrons can be captured in (n, γ), (n, α) or (n, ρ) reactions. The (n, γ) reactions may be followed by radioactive decay to produce new chemical species. In practice, however, the (n, α) reaction is by far the most important because of the insolubility of helium and thus its propensity for nucleating creep voids.

The quantities of helium produced vary from ~30 ppm in LWR cladding to nearer 100 ppm in LMFBR cladding after 500 days [110]. By way of comparinon, several thousand ppm are expected in the first wall of the fusion reactor due to the 3.5 MeV α-particles produced by the D-T reaction and the increased (n, α) cross-section at high neutron energies. At moderate temperatures, the helium atoms are mobile and agglomerate into bubbles which contribute to radiation hardening, but the effect is small compared with displacement hardening. Any increase in susceptibility to LME will therefore also be small. As the temperature increases, however, the bubbles coarsen and migrate to the grain-boundaries, nucleating cavities which severely limit both short-term and creep ductility. This limitation is marked above 650°C in AISI 316 stainless steel. If a liquid metal which caused embrittlement at high temperatures was present, then some cooperative interaction seems almost certain, although LME becomes less likely as the temperature increases. It is worth noting in passing that a similar grain boundary segregation of other transmutation products or even normal impurities could in principle be caused by the sweeping of point-defects to grain-boundary sinks.

4.2.2. *Transmutation by fission*

In contrast to the limited range of transmutation products arising from neutron capture by non-fissile elements, the fission process creates a variety of new elements distributed around mass numbers 96 and 139. Mixed oxide fast reactor fuels are designed to achieve a burn-up of 10% and therefore contain 20% fission products at the end of their life. Fig. 13 shows the predicted yield [111]. Yields are only slightly

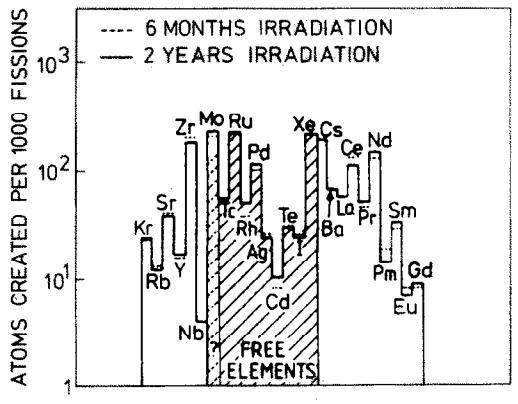

Fig. 13. Proportion of fission-products in mixed oxide fast reactor fuel (after Leitnaker [111]).

affected by neutron energy, but the light peak is shifted upwards for plutonium compared to uranium fission [112]. The removal of heavy-metal atoms releases oxygen and the chemical state of the fission product is determined by the oxygen-potential of the fuel at a given temperature and burn-up. It is estimated that after 2 years irradiation, the elements in the shaded region of fig. 13, i.e., molybdenum to xenon, will exist in the free state; the remainder (apart from krypton) will exist as oxides.

The possibility of LME by one of the low melting-point products (caesium, cadmium, tellurium) will depend to some extent on the quantities available. A simple calculation for a typical fast reactor fuel pin suggests that a few milligrams of cadmium might be present. Although such amounts are small, post-irradiation examination shows that considerable segregation can occur, presumably under the influence of thermal gradients. Furthermore, LME failures can be caused by very small traces of the embrittler [113, 114].

Failure of cladding alloys by LME thus seems quite possible. For example, cadmium embrittles Zircaloys [115] although not AISI 302 stainless steel. It is interesting to note also that tellurium and caesium, which are produced in larger quantities than cadmium, have been associated with attack on a 20Cr/25Ni Nb-stabilized stainless steel cladding alloy [116]. However, whereas failures in Zircaloy cladding have frequently been studied as a form of stress-induced environmental embrittlement (either LME or stress-corrosion), the attack of Cs/Te mixtures on stainless steels has usually been carried out from a corrosion standpoint on unstressed samples. There is clearly a need for more work on this topic.

5. Systems susceptible to LME

This section summarises some of the available information on LME systems to provide introductory data for the analysis of environmental effects and as a guide for the avoidance of embrittling combinations. Most of the published literature describes embrittlement by nominally pure liquid metals, whereas the embrittled solids include alloys and pure metals. To simplify the presentation, therefore, the information is catalogued according to the liquid metal. As a further restriction, only structural metals such as steels and zirconium alloys are included. The main emphasis is placed on the identification of systems with positive reports of LME. A lack of information for any given system should not be interpreted as indicating immunity. More complete lists of references have been published in a recent review [117] and a bibliography is kept up-to-date at Harwell [118].

Antimony

Carbon, silicon and chromium steels are reported to crack during bending in contact with antimony at 1000–1200°C [119], but these temperatures are rather high in relation to the antimony melting point (630°C) and would not constitute the most severe conditions for LME. A clearer indication of the embrittling potency of antimony is given by its effect as an alloying addition to lead [38]. This correlates with the low positive heat of mixing quoted in table 2.

Bismuth

Few experimental results are available, but the heat of mixing of the iron–bismuth system is similar to that of the iron–lead system and several ferrous alloys suffer LME by lead (table 2). Also, the Fe/Bi, Fe/Pb and Fe/Cu systems all show positive deviations from Raoultian behaviour and are therefore considered to be likely to embrittle [55]. These indications are partially confirmed by reports of the effect of molten bismuth on the ductility of three heat-treated alloy steels [3]. Both notched and smooth mild steel specimens are embrittled at 250 and 460°C [2]. The embrittlement of AISI 4140 at 370°C is increased by additions of bismuth to lead [8], but a quenched and tempered constructional steel was not embrittled in bismuth at 300°C [15].

Cadmium

Several steels are embrittled by pure liquid cadmium at 350°C [120], which is more effective than bismuth and lead, but less effective than solder and tin [3].

The embrittlement of Zircaloy-2 by cadmium has been investigated in connection with cladding failure in LWR fuel elements. Mechanical interaction between the UO_2 fuel pellets and the cladding gives

Table 4
Steels tested for embrittlement by cadmium plating [32]

Steel	Yield stress (MPa)	C	Mn	P	S	Si	Ni	Cr	V
AISI 4340	1660	0.41	0.79	0.013	0.015	0.28	1.66	0.85	–
AISI 1095	1380	1.05	0.42	0.028	0.026	0.16	–	–	–
AISI 4130	1520	0.28	0.51	0.021	0.018	0.26	–	0.86	–
AISI 302	317	0.10	1.05	0.018	0.016	1.00	8.42	17.9	–
H-13	1465	0.52	0.35	0.027	0.007	1.09	1.53	5.1	1.0

rise to stresses which cause failure under the combined action of embrittling fission products, specific mechanical loading conditions, and irradiation hardening [121]. Background laboratory experiments showed that embrittlement was caused by solid cadmium at 300°C, liquid cadmium at 340°C or cadmium dissolved in caesium at either temperature [115]. Fracture was transgranular with quasi-cleavage facets and substantially no reduction in area (RA), whereas about 75% RA was observed in caesium alone at 300°C.

Solid cadmium is also an effective embrittler and causes cracking in titanium alloys and steels. Kennedy has reported tensile, stress-rupture, fatigue and impact properties on the range of cadmium-plated aircraft steels in table 4 [32]. Initial experiments established that the embrittlement observed was not due to hydrogen pick-up during plating nor to chemical attack by cadmium in the absence of stress. The 4340, 4130 and 1095 steels were all embrittled in the quenched and tempered (Q and T) high strength, condition, but not when annealed. The 4340, 4130 and H-13, but not the 1095, steels were also embrittled in stress rupture, but the embrittlement ceased below 200°C. The austenitic steel showed no embrittlement; it is interesting to note that its yield strength is similar to those of the annealed steels, which were also unaffected. The fatigue strength of the 4340 and 4130 steels was reduced. A few impact tests on the 4340 showed no effect, possibly because the cadmium supply could not follow the rapid fracture.

Slow crack growth-rates of 1.5 mm in 20 h at 300°C have been observed in 4340 steel stressed to 90% of the yield stress at temperature in contact with solid cadmium [33]. A threshold UTS of 1260 MPa was required before cracking occurred. Both transgranular and intergranular cracks were observed, but vacuum-melted specimens showed less intergranular fracture than those melted in air.

Caesium

Caesium is of direct interest to nuclear technology because it is one of the more abundant fission products and thus comes directly in contact with fuel cladding. Table 2 suggests that it should be less likely to embrittle ferrous metals than sodium, but there is little experimental information available. Early tests on a range of metals, including carbon and austenitic steels, found no evidence of LME [112]. More recent investigations have concentrated on the corrosion aspects of attack on stainless-steel cans for oxide fuels [116,123]. The data are of limited relevance to LME because of the high test temperatures (up to 800°C) and either static or zero stresses.

In contrast, LME by caesium has been studied in detail as a failure mechanism in Zircaloy cladding. Cox [124] reports embrittlement in simple bend tests at 30°C, but it was difficult to achieve reproducible wetting. Non-wetted specimens were not embrittled, even when fully immersed in the liquid metal. Confirmatory results by Wood [125] showed that precracked specimens were embrittled in dynamic tests from 30–225°C, suggesting that rapid strain is necessary to break the oxide films and permit wetting. The upper limit of 225°C indicates a brittle/ductile transition and explains the lack of embrittlement at 300°C [115]. Contradictory reports of high

temperature (300°C) embrittlement relate to deoxidised Cs–0.1 wt% Fe solutions and thus require some clarification [126].

Copper

The data in table 2 imply that copper is likely to embrittle ferrous alloys, but direct experimental evidence is limited. There are, however, numerous reports of surface cracking of ingots by copper-rich liquid phases during hot-rolling although the picture is complicated by the presence of other segregants [127]. Also, mild steel is cracked by pure copper in simple bend tests [128]. The elongation and reduction in area of mild steel wrapped with copper wire falls to zero above 1100°C [129]. The austenitic AISI 304, 316, 321 and 347 stainless steels, as well as 4340, 4140 and cobalt-based alloys are embrittled by copper plates as thin as 0.1 μm [4,113]. A ferritic type AISI 430 was unaffected.

Gallium

Although gallium is reported not to embrittle high strength titanium alloys nor a quenched and tempered constructional steel in slow bending at 34°C [15], LME was observed in notched mild steel at 34°C [2].

Indium

Some, but not all, ferrous alloys can be embrittled by both the liquid and solid indium. Armco iron was not embrittled at 160°C and strain rates of 1.7×10^{-3} and 17×10^{-3}/s; in contrast, an AISI 4140 steel was embrittled [8]. More detailed information is given by Shunk for pure iron, AISI 1040 and AISI 1095 steels in varying conditions of heat treatment [5]. The results for the iron and spheroidized steels were unusual in that the temperatures of the onset of embrittlement varied according to the strength of the alloy and the interparticle spacing in the steels. The maximum embrittlement occurred at 350 ± 25°C and the brittle/ductile transition fell in the range 390 to 415°C. In most LME systems, the onset temperature appears to be related to the melting point of the embrittler, but these results show that the behaviour of more complex two-phase materials can be significantly different. Major differences were also observed between the behaviour of steels in the spheroidized and lamellar condition. The lamellar 1095 steel was also embrittled at temperatures as low as 110°C.

Lead

Results from detailed investigations of several steels wetted with lead [7,8,29,38,39] contradict earlier claims that ferrous alloys are not susceptible [15,120,130,131]. The embrittlement begins about 100–150°C below the embrittler melting point and increases with temperature, becoming much more severe when the lead melts. A well-defined ductility-trough is often observed. Additions of antimony, bismuth, copper, tin and zinc to the lead all increase the embrittlement, whether measured by ductility or brittle/ductile transition temperature [8]. Both cold-work and grain-boundary segregation also influence the extent of embrittlement [44,45].

The use of lead additions to improve the machining properties of steels has led to failures of jet engine compressor discs, die blocks, gear teeth and steel shafts at 280–400°C and stresses approaching yield. The embrittlement is similar to LME by externally applied lead and occurs with several low-alloy Ni/Cr and Cr/Mo steels. Additions of 0.1% rare-earth metals eliminate embrittlement. Microprobe analysis shows that cerium is associated with the lead inclusions, but the mechanism of the suppression is not known in detail [7,132].

Lithium

Lithium is reported to embrittle several metals, including copper, nickel and iron alloys [50] but in some cases the degradation is caused by mechanisms other than LME [81]. The relatively high solubility of carbon and nitrogen in lithium, together with the formation of a stable nitride and carbide [133] causes corrosion of some steels [134,135]. The report of stress-dependent delayed failure of an AISI 4130 steel in lithium at 200°C [15] must therefore be regarded with caution, especially since grain boundary penetration of Armco iron is also strongly stress-dependent [13]. Work at Harwell has shown that significant surface decarburization can occur in mild steel even during short-term tensile tests (fig. 14), with intergranular failure following the decarburized grain boundaries [136]. These observations provide additional insight into reports of reductions in ductility of notched mild steel specimens in lithium at 250°C [137]. In contrast, 9 wt% Cr–1 wt% Mo and 2.25 wt% Cr–1 wt% Mo steels are much less affected, presumably because chromium and molybdenum

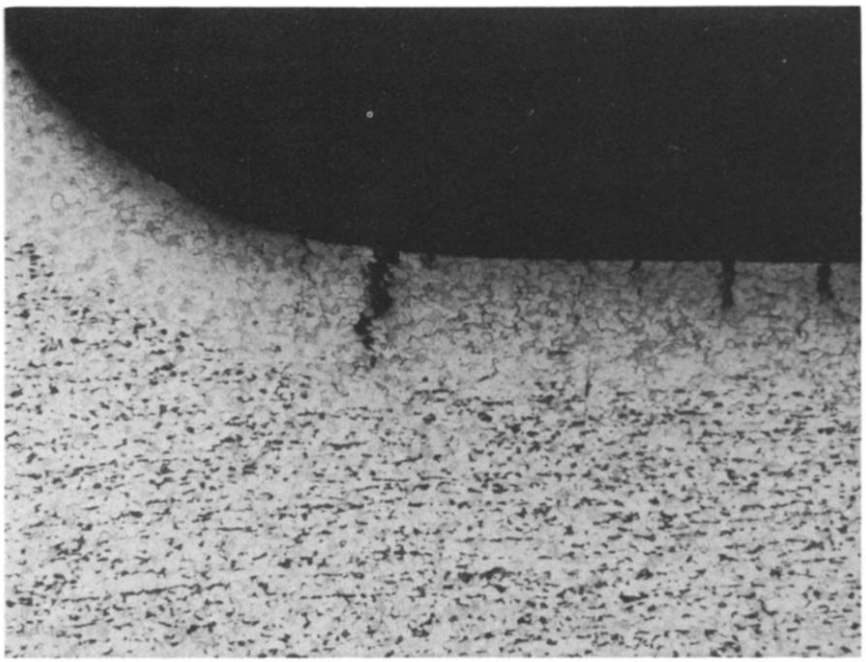

Fig. 14. Grain-boundary decarburization and cracking of a mild steel tested in lithium. Magn. X 50.

carbides are not decomposed by lithium. This supposition is supported by Harwell experiments which show no LME in high purity iron (0.007 wt% C) or in a reactor-grade AISE 316 (fig. 15).

Despite the complications introduced by corrosion attack, there is also evidence that lithium can cause "genuine" LME in some alloys. Early reports of transgranular brittle fracture in Fe–3 wt% S [138] have been confirmed during current programmes at Harwell. Fig. 16 shows both transgranular and intergranular failure in a specimen tested at 250°C and 10^{-3}/s. This embrittlement of some alloys but not

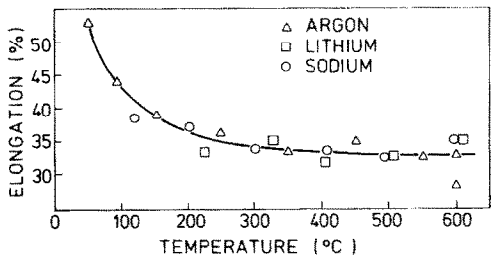

Fig. 15. Tensile ductility of annealed AISI 316 in lithium, sodium and argon.

others is similar to the action of mercury, and thus suggests that the Li/Fe system is also on the borderline of embrittlement.

Mercury

Mercury is reported to embrittle titanium alloys, pure zirconium and Zircaloys, but not steel [15,124, 139]. Considerable plastic deformation in bending occurred before failure in zirconium, and large areas of the fracture were ductile. Cracking was essentially transgranular on or near the basal plane, and characteristic fluted regions were identified with the plastic mode. In contradiction to early reports, other researchers have found LME of ferrous alloys by mercury under slightly different circumstances. As with gallium, the presence of a notch promotes LME by mercury in a low carbon steel [2]. In addition, the fracture toughness of a heat-treated Cr–Mo steel was reduced by more than an order of magnitude.

Alloys of pure iron with more than 2 wt% Si or 4 wt% Al are also embrittled. The effects of the solute were correlated with an increased grain-size dependence of the flow stress, and a change from fine diffuse, wavy slip to coarse planar slip [36]. Similar

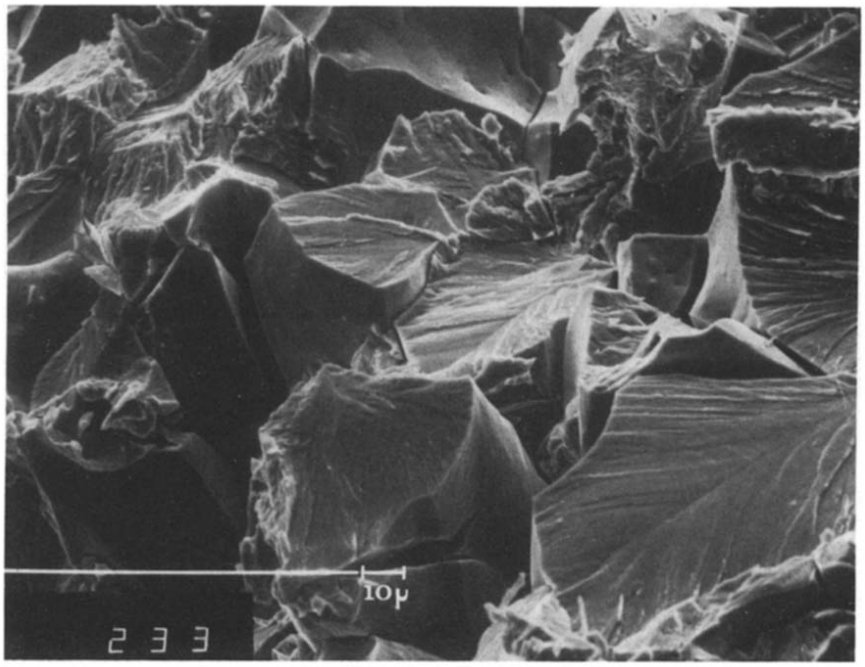

Fig. 16. Transgranular and intergranular fractur in Fe–3 wt% Si tested in lithium at 247°C and 1.3×10^{-2}/s.

behaviour was seen in Fe–Ni alloys in mercury–0.1 wt% indium [75]. Above 7 wt% Ni, the ductility of smooth annealed specimens in mercury fell progressively, although the yield stress and UTS remained unchanged. The COD and strain-energy release rate, G_c, in the mercury solution peaked at about 7 wt% Ni although the G_c values were still about an order of magnitude less than those in air. The significance of the nickel content was attributed to changes in slip behaviour as the structure changed from ferritic to martensitic at about 7%.

Rubidium

It has been suggested that rubidium embrittles notched specimens of monel 400 at 127°C and 10^{-6}/s [140], but the detailed results show that the flow-stress was reduced by about 50% before fracture. This is not a usual effect of LME and further clarification is therefore required.

Sodium

The possibility of LME of steels and other structural alloys by sodium is of interest to LMFBR technology, especially inview of the empirical correlations in section 2.7 which imply that the Fe/Na system should be susceptible and the recent assertion that LME of steels by sodium is well-documented [51]. However, the latter statement refers to fatigue tests carried out over extended periods in oxygen-contaminated sodium [141]. The results were originally interpreted as indicating a corrosion-fatigue process and this explanation would still apear to be valid. It has, in fact, been suggested that the scavenging action of clean sodium provides a less damaging environment that air [142,143]. Furthermore, an extensive search of the open literature, major data compilations, and reports from international laboratories, together with operating experience of sodium-cooled reactors, shows no evidence of LME.

Nevertheless, this information, although convincing, is largely circumstantial. There are few results directly relevant to LME because most reports refer to mechanical tests on specimens which have been cleaned following prior exposure to the liquid metal. In the few tests carried out in contact with sodium, mild steel showed no embrittlement at 150 and 250°C [130]. Similarly Yagee and Gilbert were able to bend AISI 304 through angles of 90–140° about a

radius of 4 × thickness at 300°C without cracking [144]. Experiments at Harwell have also found notched samples of AISI 316 and mild steel to be ductile in sodium at 200, 400 and 600°C [136]. In push-pull fatigue, sodium had no detrimental effect on a 1.1 wt% Cr steel at 150°C [145].

These findings lend support to the figures shown in table 2, which imply that sodium and caesium are likely to be the weakest embrittlers of ferrous alloys. However, such estimates must be treated with caution because a similar relationship exists with copper and aluminium alloys. In this case, however, sodium does embrittle copper if it has been hardened with 5 wt% Al [81] and is also reported to embrittle unspecified aluminium alloys [15].

Tellurium

Rostoker et al. [15] found that tellurium embrittled an alloy constructional steel in bending at 475°C. Apart from this one report, there appears to be no other work on LME by tellurium alone, although several workers have considered the corrosive effects of fission-product mixes including tellurium on canning materials. The mechanism of attack is complicated because, like lithium, tin, and zinc, tellurium is chemically reactive towards structural materials such as iron, nickel and chromium.

Studies in connection with the molten salt reactor found that vapour-deposited tellurium on Hasteloy N (a Ni/Mo/Fe/Cr alloy) at 400°C caused extensive surface cracking when the specimens were tested at 25°C after exposure [146]. Further tests on Hasteloy N, AISI 304 and Inconel 601 exposed to fission products under irradiation for 1145 h at 700°C showed that Hasteloy was most degraded with the reduction in area falling from 30 to 17%. The degradation was attributed to grain-boundary attack with the formation of nickel tellurides. Broadly similar results are reported for the attack of tellurium/caesium mixtures on AISI 316 [116,123]. The creep rupture life of 20 Cr/25 Ni Nb-stabilised stainless steel in tellurium at 750°C was reduced by more than half and the creep strain from 60 to about 15%, but the tensile properties after exposure were only slightly reduced [147]. The effect of tellurium appeared to be greatest under the combined action of stress and the environment, an observation which is consistent with LME.

Tin

Tin and tin–lead solders embrittle a variety of chromium and austenitic steels at 316°C [3]. More detailed experiments on low-alloy AISI 4140 and 4145 steels showed that tin also embrittled when solid [29] and increased the potency of lead [38]. It was further shown that embrittlement of an AISI 3340 steel by tin was unaffected by segregation of tin and arsenic dopants, but slightly alleviated by segregation of phosphorus [45]. Tanaka and Fukunaga report embrittlement of mild steel in both smooth and notched specimens [130] and quote reductions in ductility of about 50% in smooth specimens at 350°C and 10^{-3}/s. A return to ductility was observed at about 450°C. The fatigue properties of mild steel are also degraded, giving a lower S-N curve and an increased tendency to intergranular fracture [148, 149].

Zinc

Embrittlement of stainless steels by zinc was much discussed in the literature following the Flixborough explosion [114,150,151]. Some additional information was generated during this period, but the mechanisms of the different modes of attack are still not clear. Three temperature regimes were identified in the attack on an unstressed 18/8 austenitic alloy [12, 152]. From 419–570°C, the steel was slowly eroded, and from 570–750°C, an intermetallic Ni–Zn compound was formed. Above 750°C, grain boundary penetration occurred and the denudation of nickel led to a $\gamma \rightarrow \alpha$ phase transformation. The stress associated with the accompanying volume change promoted slow cracking along the grain boundaries. However, fast fracture has also been observed in stressed AISI 316 above 790°C. An onset temperature so far above the melting point of the embrittler is unusual in LME and suggests that more complicating factors are involved.

Conventional LME by zinc occurs in mild steel but the influence of a holding period before testing and of surface finish require further study [130]. In addition, an AISI 4140 steel quenched and tempered to 1400 MPa UTS was embrittled by solid zinc [29].

6. Concluding remarks

This review has attempted to establish common ground between the factors which influence liquid

metal embrittlement and the property changes and materials met in nuclear applications. The survey has been concerned with general trends rather than specific data because more detailed discussions already exist in the literature; on the nuclear aspects in particular, it is not possible to treat fully in a few paragraphs topics which themselves merit comprehensive reviews. In addition, there is little overlap in materials data between LME and nuclear studies, presumably because the considerable experience with both active and inactive pilot plants has shown that LME is not a practical problem.

Nevertheless, laboratory data demonstrate unequivocally that structural alloys used in nuclear plant can suffer LME and, conversely, that some metals used as nuclear coolants or arising as fission products can cause LME. Clearly, therefore, it must be evaluated as a potential cause of failure when selecting new materials, when specifying permissible materials combinations for designers and operators, and when analysing component failures. In particular, tests should be designed to highlight any tendency to embrittlement; results from corrosion tests under static loads may be misleading.

Some factors peculiar to the nuclear environment must also be considered. Because LME is generally a low-temperature phenomenon, frequently with clearly-defined limits, it is unlikely that there will be any synergistic effects with creep cavitation failure. On the other hand, its similarity to elastic fracture suggests that radiation hardening and the presence of certain fission products may be detrimental. It would be informative and not unduly difficult to check these speculations, using carefully-chosen systems.

Acknowledgements

Grateful thanks are due to many colleagues who offered specialist advice on various aspects of radiation damage, and particularly to Mr. S.F. Pugh for helpful discussions and comments on the manuscript.

References

[1] A.K. Huntington, J. Inst. Met. 11 (1914) 108.
[2] M. Tanaka and H. Fukunaga, in: Proc. 12th Jap. Congr. on Materials Res., Kyoto, 1969, p. 248 (see J. Soc. Mater. Sci. Jap.).
[3] G. Wesley-Austin, J. Inst. Met. 58 (1936) 173.
[4] W.F. Savage et al., Welding 57 (1978) 9s.
[5] F.A. Schunk, Thesis, see Dissertation Abstr. B37 (1976) no. 76-23501.
[6] E.G. Coleman et al., Acta. Met. 9 (1961) 491.
[7] W.R. Warke and N.N. Breyer, J. Iron Steel Inst. 209 (1971) 779.
[8] 3rd Prog. Report. to US Army, Project Themis (AD-908377).
[9] J.E. Cantwell and R.E. Bryant, Hydrocarbon Processing, May (1973) p. 114.
[10] Brit. Eng. Tech. Reports. 6 (1965) 76; 7 (1966) 42; 11 (1972) 63.
[11] The Observer (Oct. 10th 1976) p. 3.
[12] M. Andreani et al., Compt. Rend. (Paris) 263 (1966) 1041.
[13] W. Jordan et al., Nucl. Technol. 39 (1978) 75.
[14] G.I. Denshchikova et al., Soviet Mater. Sci. 11 (1973) 5.
[15] W. Rostoker et al., Embrittlement by Liquid Metals (Rheinhold, New York, 1960).
[16] M.H. Kamdar and A.R.C. Westwood, Environment Sensitive Mechanical Behaviour, Eds. A.R.C. Westwood and N.S. Stoloff (Gordon and Breach, 1966) p. 581.
[17] A.R.C. Westwood et al., Trans. ASM 60 (1967) 723.
[18] C.F. Old and P. Trevena, Met. Sci. J. 13 (1979) 591.
[19] H. Nichols and W. Rostoker, Trans. AIME 224 (1962) 1258.
[20] A.R.C. Westwood et al., Fracture, Vol. 3, Ed. H. Leibowitz, (Academic Press, 1971) p. 589.
[21] P.C. Hancock and M.B. Ives, Can. Met. Quart. 10 (1971) 207.
[22] G.L.J. Bailey and H.C. Watkins, J. Inst. Met. 80 (1951/52) 57.
[23] R.J. Klein-Wassink, J. Inst. Met. 95 (1967) 38.
[24] M. Barlow and P.J. Planting, Z. Metallk. 60 (1969) 719.
[25] M. Barlow and P.J. Planting, Z. Metallk. 60 (1969) 817.
[26] C.F. Old, AERE-R9043 (1978).
[27] N.S. Stoloff and T.L. Johnston, Acta Met. 11 (1963) 251.
[28] N.S. Stoloff, Surfaces and Interfaces, Vol. II, Eds. J.J. Burke et al. (Syracuse University Press, 1968) p. 157.
[29] J.C. Lynn et al., Mater. Sci. Eng. 18 (1975) 51.
[30] D.A. Meyn, Corrosion 29 (1973) 192.
[31] D.N. Fager and W.F. Spurr, Corrosion 26 (1970) 409.
[32] E.M. Kennedy, WADD Tech. Report. 60-486 (1961).
[33] D.N. Fager and W.F. Spurr, Corrosion 27 (1971) 72.
[34] C.F. Old and P. Trevena, Met. Sci. J. 13 (1979) 487.
[35] A.P. Savitskii and L.K. Savitskaya, Soviet Phys. Doklady, 12 (1967) 647.
[36] N.S. Stoloff et al., Environment Sensitive Mechanical Behaviour Eds. A.R.C. Westwood and N.S. Stoloff (Gordon and Breach, 1966) p. 613.
[37] C.M Preece and A.R.C. Westwood, in: Proc. 2nd. Intern. Conf. on Fracture, Brighton, 1969, Ed. P.L. Pratt (Chapman and Hall, London).
[38] N.N. Breyer and K.L. Johnson, J. Testing Evaluation 2 (1974) 471.

[39] N.N. Breyer, private communication.
[40] M.H. Kamdar, Progr. Mater. Sci. 15 (1973) 289.
[41] R. Rosenberg and I. Cadoff, Fracture of Solids (Interscience, 1963) p. 607.
[42] C.M. Preece, Research/Development, Oct. 1972, p. 30.
[43] H. Nichols and W. Rostoker, Trans. Met. Soc. AIME 230 (1964) 251.
[44] N.N. Breyer and M. Watkins, in: 3rd Prog. Report to US Army, Project Themis (AD908377).
[45] S. Dinda and W.R. Warke, Mater. Sci. Eng. 24 (1976) 199.
[46] L.P. Costas, Corrosion 31 (1975) 91.
[47] D.A. Meyn, Fractography in Failure Analysis, ASTM STP645, Eds. B.M. Strauss and W.L. Cullen (Am. Soc. for Testing and Materials, 1978) p. 49.
[48] N.J. F. Gunn et al., RAE Tech. Memo Mater. 233 (1975).
[49] T.M. Regan and N.S. Stoloff, Met. Trans. 8A (1977) 885.
[50] F.A. Shunk and W.R. Warke, Scripta Met. 8 (1974) 519.
[51] N.S. Stoloff, Symp. on Environment Sensitive Fracture of Engineering Materials, Chicago, 1977.
[52] M.J. Kelley and N.S. Stoloff, Met. Trans. 6A (1975) 159.
[53] W.M. Robertson, Trans. AIME 236 (1966) 1478.
[54] G.S. Knizhnik, Nauchn. Tr. Vses. Zaoch. Machinostroit. Inst. 12 (1975) 79.
[55] M.I. Chaevski, Soviet Mater. Sci. 1 (1965) 433.
[56] M.I. Chaevski and V.V. Popovich, Soviet Mater. Sci. 2 (1966) 102.
[57] S.P. Lynch, Fracture 1977, Vol. 2, Ed. D.M.R. Taplin (Univ. of Waterloo, Waterloo) p. 859.
[58] S.P. Lynch, Scripta. Met. 13 (1979) 1051.
[59] J.R. Weeks, in: Proce. NASA/AEC Liq. Metals Corrosion Meeting (NASA, Washington, DC, 1963) p. 97.
[60] E.D. Shchukin and V.S. Yushchenko, Soviet Mater. Sci. 2 (1966) 95.
[61] V.M. Zalkin, Soviet Mater. Sci. 4 (1968) 18.
[62] W.M. Robertson, Met. Trans. 1 (1970) 2607.
[63] F.N. Rhines et al., Trans. ASM 55 (1962) 22.
[64] M.O. Speidel and M.V. Hyatt, Advan. Corrosion Sci. Technol., Eds. Fontana and Staehle (Plenum, New York, 1972) Vol. 2, p. 115.
[65] R.A. Oriani and P.H. Josephic, Acta Met. 22 (1974) 1065.
[66] N.J. Petch, Fracture, Proc. Swampscott Conf., Eds. B.L. Averbach et al. (Wiley, 1959) p. 54.
[67] A.H. Cottrell, Trans. AIME 212 (1958) 192.
[68] H. Ichinose and C. Oouchi, Trans. Jap. Inst. Met., 9s (1968) 980.
[69] C.M. Preece and A.R.C. Westwood, Trans. ASM 62 (1969) 418.
[70] A.A. Griffith, Phil. Trans. Roy. Soc. (London) 221A (1920/21) 163.
[71] A.N. Stroh, Advan. Phys. 6 (1957) 418.
[72] J.D. Eshelby et al., Phil. Mag. 42 (1951) 351.
[73] U.N. Nanda, Thesis (Illinois Inst. of Technol., 1973).
[74] H. Ichinose and C. Oouchi, Trans. Jap. Inst. Met. 10 (1969) 174.
[75] H.W. Hayden and S. Floreen, Phil. Mag. 20 (1969) 135.
[76] M.M. Shea and N.S. Stoloff, Mater. Sci. Eng. 12 (1973) 245.
[77] D. McLean, J. Phys. Radium 36 (1975) C4-273 (Intern. Colloq. on Grain-Boundaries in Metals, St. Etienne, 1975).
[78] W.R. Tyson, Can. Met. Quarterly 14 (1975) 307.
[79] A.R. Miedema and R. Boom, Z. Metallk. 69 (1978) 183.
[80] A.S. Tetelman and S. Kunz, Tech. Report. DAHC-04-69-C-0008, UCLA.
[81] C.F. Old and P. Trevena, in: Proc. 3rd Intern. Conf. on Mechanical Behaviour of Materials. Cambridge, 1979, Eds. K.J. Miller and R.F. Smith (Pergamon Press, 1979) Vol. 2, p. 397.
[82] A.R. Miedema and F.J.A. den Broeder, Z. Metallk. 70 (1979) 10.
[83] E.A. Little, Intern. Met. Rev. 21 (1976) 25.
[84] M.W. Thompson, Defects and Radiation Damage in Metals (Cambridge University Press, 1969).
[85] A.H. Cottrell, Theoretical Structural Metallurgy (Arnold, London, 1957).
[86] S.N. Buckley, Properties of Reactor Materials and Effects of Radiation Damage, Ed. W.J. Littler (Butterworths, London, 1963).
[87] D.O. Northwood, At. Energy Rev. 15 (1977) 547.
[88] S.N. Buckley, AERE-R5944 2 (1968) 547.
[89] V. Fidleris, At. Energy Rev. 13 (1975) 51.
[90] J.E. Harbottle and R.M. Cornell, Nucl. Eng. Design 42 (1977) 423.
[91] D.R. Harries, Nucl. Energy 17 (1978) 301.
[92] R. Bullough, in: Proc. Intern. Conf. on Fundamental Aspects of Radiation Damage in Metals, Gatlinburg, TN, 1975, USERDA, p. 1261.
[93] D.R. Harries, J. Nucl. Mater. 65 (1977) 157.
[94] B. Watkins and D.S. Wood, Applications – Related Phenomena in Zirconium, ASTM STP 458 (Am. Soc. for Testing and Materials, 1969) p. 226.
[95] E.R. Gilbert et al., J. Nucl. Mater. 65 (1977) 266.
[96] R.A. Murgatroyd and A. Rodgerson, J. Nucl. Mater. 79 (1979) 302.
[97] D.G. Hardy, Irradiation Effects on Structural Alloys for Nuclear Reactor Applications, ASTM STP 484 (Am. Soc. for Testing and Materials, 1970) p. 215.
[98] R.C. Perrin, private communication.
[99] M.J. Makin et al. in: Proc. 2nd UN Intern. Conf. on Peaceful Uses of Atomic Energy, Geneva, 1958, Vol. 5, p. 446.
[100] E.R. Nichols and D.R. Harries, Symp. on Radiation Effects and Neutron Dosimetry, ASTM STP 341 (Am. Soc. for Testing and Materials, 1962).
[101] R.A. Wullaert et al., Irradiation Effects on Structural Alloys for Nuclear Reactor Applications, ASTM STP 484 (Am. Soc. for Testing and Materials, 1970) p. 20.
[102] K.R. Garr and A.G. Pard, Irradiation Effects on the Microstructure and Properties of Metals, ASTM STP 611 (Am. Soc. for Testing and Materials, 1976) p. 72.
[103] R.L. Fish and J.D. Watrous, ibid., p. 91.
[104] R.L. Fish and C.W. Hunter, ibid., p. 119.

[105] A.L. Ward et al., ibid., p. 156.
[106] D.R. Harries, J. Nucl. Mater. 82 (1979) 2.
[107] E.E. Bloom and F.W. Wiffen, J. Nucl. Mater. 58 (1975) 171.
[108] M.S. Weschler et al., Acta Met. 17 (1969) 541.
[109] J.V. Sharp, AERE-R7006 (1972).
[110] D.R. Olander, Fundamental Aspects of Nuclear Reactor Fuel Elements, TID-26711-P1, USERDA (1976).
[111] J.M. Leitnaker, J. Nucl. Mater. 51 (1974) 95.
[112] J.H. Davies and F.T. Ewart, J. Nucl. Mater. 41 (1971) 143.
[113] W.F. Savage et al., Welding J. 57 (1978) 237s.
[114] A.H. Cottrell and P.R. Swann, The Chemical Engineer (April 1976) p. 266.
[115] W.T. Grubb and M.H. Morgan, Proc. ANS Topical Meeting on Water Reactor Fuel Performance, St. Charles, IL, 1977.
[116] J.F. Antill and J.B. Warburton, J. Nucl. Mater. 71 (1977) 134.
[117] M.G. Nicholas and C.F. Old, J. Mater. Sci. 14 (1979) 1.
[118] M.G. Nicholas et al., AERE-R9199 (1978) and supplement (1979).
[119] H. Schottky et al., Arch. Eisenhütternw. 4 (1931) 541.
[120] W. Radeker, Werkstoffe und Korrosion 24 (1973) 851.
[121] L.F. Coffin and R.P. Gangloff, Proc. ANS Topical Meeting on Water Reactor Fuel Performance, St. Charles, 1977.
[122] M.D. Chadwick et al., IRD 64-55 (1964) and IRD 65-57 (1965).
[123] P.S. Maiya and D.E. Busch, Met. Trans. 6A (1975) 409.
[124] B. Cox, Corrosion 28 (1972) 207.
[125] J.C. Wood et al., J. Nucl. Mater. 57 (1975) 155.
[126] B.C. Syrett et al., Zirconium in the Nuclear Industry, ASTM STP633, Eds. A.L. Lowe and G.W. Parry (Am. Soc. for Testing and Materials, 1977) p. 281.
[127] D.A. Melford, J. Iron Steel Inst. 200 (1962) 290.
[128] R. Genders, J. Inst. Met. 37 (1927) 215.
[129] V.L. Kolmogarov, Russ. Met. Fuels 1 (1976) 61.
[130] M. Tanaka and H. Fukunaga, J. Soc. Mater. Sci. Japan 18 (1969) 411.
[131] W. Herrnkind, in: Proc. 3rd Intern. Conf. on Lead, Venice, 1968, p. 387.
[132] N.N. Breyer, 1973 Electric Furnace Proc., Met. Soc. AIME.
[133] G. Long, in: Proc. BNES Conf. on Liquid Alkaline Metals, Nottingham, 1973, p. 31.
[134] D.L. Olson and W.L. Bradley, in: Proc. Intern. Conf. on Liquid Metal Technology in Energy Production, 1976, USERDA, p. 446.
[135] J.E. Selle, ibid., p. 453.
[136] C.F. Old and P. Trevena, AERE-R9505 (1979).
[137] J.E. Cordwell, in: Proc. BNES Conf. on Liquid Alkali Metals, Nottingham, 1973, p. 177.
[138] H. Nichols and W. Rostoker, Acta Met. 9 (1961) 504.
[139] I. Aitchison and B. Cox, Corrosion 28 (1972) 83.
[140] T.R. Pinchback, TREE 1291 (1979).
[141] J.K. Beddow, Metallurgia 77 (1968) 185.
[142] L.A. James, Scripta Met. 10 (1976) 1039.
[143] L.H. Kirschler and R.C. Andrews, J. Basic Eng. 91 (1969) 785.
[144] F.L. Yagee and E.R. Gilbert, IAEA Symp. on Alkali Metal Coolants, Vienna, 1966.
[145] J.W. Martin and G.C. Smith, private communication.
[146] L.E. McNeese, ORNL-5047 (1975).
[147] R.C. Lobb, Mater. Sci. Eng. 36 (1978) 165.
[148] J.W. Martin and G.C. Smith, Metallurgia 54 (1956) 227.
[149] M. Tanaka and H. Fukunaga, Sci. Rept. Osaka Univ. (Japan) 19 (1970) 43.
[150] D. Elliott, Process Engineering, July 1976, p. 67.
[151] J.G. Ball, ibid., p. 275.
[152] M. Andreani et al., Mém. Sci. Rev. Mét. 66 (1969) 21.